EFFECTS OF ELECTROLYTE FLOW ON THE PERFORMANCE OF LEAD–ACID CELLS

J. DORIA*, M. C. DE ANDRÉS and C. ARMENTA

Grupo de Energía Solar, Fac. Físicas, Universidad Complutense, 28040 Madrid (Spain)

J. FULLEA and F. GRAÑA

FEMSA Batteries R&D, C/Hnos G^a Noblejas 19, 28037 Madrid (Spain)

(Received September 25, 1986; in revised form June 18, 1987)

Summary

Charging processes in lead–acid batteries cause a typical "multilayer" configuration due to stratification in the electrolyte as sulphuric acid is generated. In consequence a voltage gradient is formed between the bottom and the top of the cell and the efficiency and performance are reduced. Modern methods of mixing the solution, by using compressed air or pumping the solution upwards, avoid stratification but introduce foreign elements. In this paper a new method of avoiding stratification by circulating sulphuric acid through a magnetic pump is presented. It gives up to about 20% higher efficiency and improved performance. This new method also saves energy when charging, especially at low charge rates.

Résumé

Les procédés de chargement des batteries de plomb–acide causent une configuration très typique étant donné la stratification de l'électrolyte lorsque l'acide sulphurique est généré. La principale conséquence est l'apparition d'un gradient de potential chimique entre le fond et la surface réduisant l'efficacité de celui-ci. Les méthodes modernes évitent ce problème par l'utilisation de l'air comprimé ou de pompes à air pour mélanger les différentes zones, mais ils présentent l'inconvénient d'introduire des éléments additionels. Le présent travail a développé l'idée d'éviter la stratification avec des pompes magnétiques de circulation pour l'électrolyte. Les résultats obtenus ont été très bons et l'efficacité augmentée.

Introduction

It has been shown that one of the most important problems in static electrical storage is a non-uniform electrolyte concentration, especially

*Author to whom correspondence should be addressed.

0378-7753/88/$3.50

during charging, which provokes a density gradient between the top and the bottom of the cell. This causes a non-uniform current distribution in the electrodes with the upper portions of the plates suffering from high current densities. At the same time the active material near the bottom suffers from being immersed in concentrated acid. Both effects tend to reduce the efficiency and the capacity of the cell [1, 2].

This problem has been avoided by overcharging the batteries at elevated potential: a technique which is still widely used. This overvoltage generates gases (hydrogen and oxygen) at both electrodes and mixing occurs to make the solution homogeneous. Nevertheless, overcharging damages the cell and reduces the cycle life [3]. The high potential also introduces the penalty of lowered energy efficiency. In recent years alternative methods of eliminating this problem have appeared. These include either pumping air into the bottom of the cell to mix the electrolyte or removing concentrated acid from the bottom to the top of the cell by means of compressed air.

In this paper the results of studies of the effect electrolyte flow has on the performance of a lead–acid cell are presented. The flow was induced by pumping the acid solution through the cell. This avoided producing or introducing any gases into the battery and gave more reliable performance test results*.

Engineering design of the electrolyte circulation device

We compared two lead–acid storage batteries, FEMSA type 3 and EAF-150-1. Both have a 150 A h discharge capacity at the ten hour rate and a maximum capacity of 240 A h at the hundred hour rate.

Holes were made in one of the batteries, one at the bottom and one at the top. The acid was pumped from the lower hole and back into the battery through the upper hole (see Fig. 1). The other battery was not modified. Both systems had very low resistance loads which were designed to maintain a constant value during the experiment and be independent of temperature. Changes can be assumed to be negligible because of the very low varying internal resistance during charge–discharge cycles. The output voltage was checked every fifteen minutes.

Influence of electrolyte circulation on charge transport

The total reaction depends on the relative speeds of the ionic transport and electron transfer, although, as the former increases, so does the latter. In many cases the general process is controlled by the charge transfer at

*We refer to static electrical storage as non-traction batteries for static applications such as photovoltaic arrays, battery backed-up instrumentation in nuclear and communications applications and hospitals, etc.

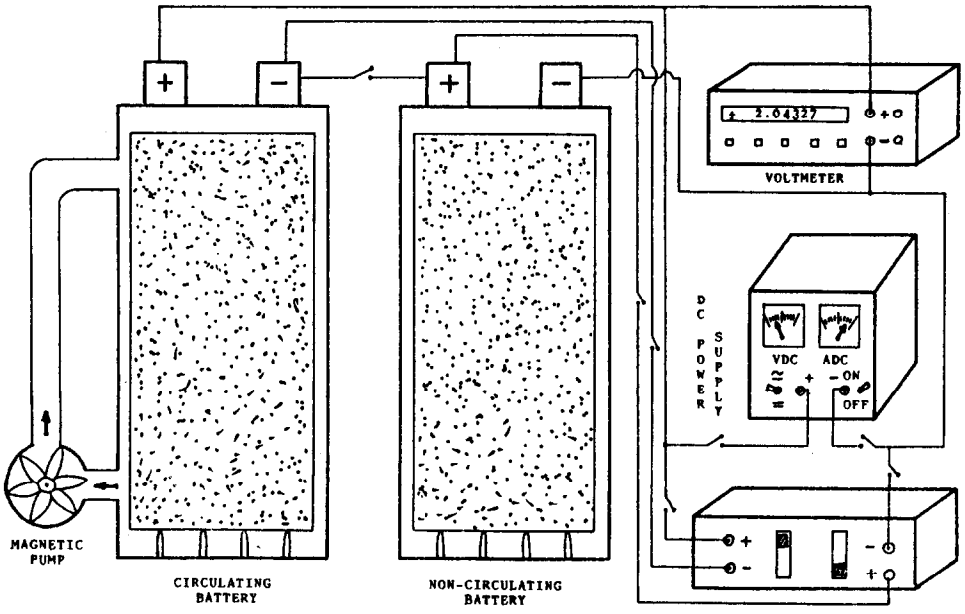

Fig. 1. Experimental device.

the double layer; usually this is called the "reaction determining step" (rds). Ionic transport can become the controlling factor, however, when it falls from its initial to a very low value. In such a case the flow charge transfer cannot supply the current exchange at the double layer and performance becomes degraded. When the total process is considered:

bulk solution	IONIC TRANSPORT	Outer Helmholtz plate	CHARGE TRANSFER	Electrode
$x \to \infty$	$\rightarrow\rightarrow\rightarrow\rightarrow\rightarrow\rightarrow\rightarrow\rightarrow$	$x = 0$	$\rightarrow\rightarrow\rightarrow\rightarrow\rightarrow\rightarrow\rightarrow$	

Given that the rds corresponds to the highest activation energy step we can see that as diffusion transport* is a kinetic process depending on the activation energy (boundary potential), charge transfer will be the rds if the activation energy for diffusion transport is low. Ionic transport could be the rds, however, if we have dilute solutions, although its activation energy would be very low.

In the general case, diffusion ionic transport, without viscous or inertial effects, is given by Fick's law [4]

$$-J_i = \sum_{k=1}^{j-1} D_{ik}(\nabla\rho_k - \rho_k s_k \nabla T) + \sum_{m=1}^{j-1} \Omega_{im}(\bar{v}_m \nabla P - \bar{F}_m + \bar{z}_m \nabla V) \qquad (1)$$
$$i = 1, \ldots, j-1$$

*Transport would also be produced by conduction and hydrodynamic flow.

where

D_{ik} : relative diffusion coefficients
F_{m} : external forces
i : solute
j : solvent
s_k : Soret coefficient
$\bar{v}_m$: partial volumes
$\bar{z}_{\mathrm{m}}$: specific charge of ionic species m
$\nabla\rho_k$: partial density gradient
Ω_{im} : phenomenological coefficients
∇P : pressure gradient
∇V : electrical potential gradient.

If the system is in thermo-mechanical equilibrium (temperature and pressure gradient and external forces equal zero) expression (1) can be rewritten as:

$$-J_i = \sum_{k=1}^{j-1} D_{ik}\,\nabla\rho_k + \sum_{m=1}^{j-1} \Omega_{im} z_{\mathrm{m}}\,\nabla V \qquad i = 1, \ldots, j-1 \tag{2}$$

Taking into account that the chemical potential depends on pressure, temperature, and partial densities (ρ_i) we can now write:

$$\mu_m = \mu_m(T, P, \rho_1, \ldots, \rho_{j-1})$$

or

$$\mu_m = \mu_m(\rho_1, \ldots, \rho_{j-1}) \qquad \text{(thermo-mechanical equilibrium)}$$

We can rearrange the previous expression as:

$$\rho_i = \rho(\mu_m)$$

and then

$$\nabla\rho_i = f(\nabla\mu_m)$$

Moreover, phenomenological coefficients (Ω_{im}) can be expressed as a function of the diffusion coefficients:

$$\Omega_{im} = f(D_{ik}, \mu_m, \rho_k)$$

and eqn. (2) can be rewritten [5]

$$-J_i = \frac{D_{ik} c_k}{RT} \frac{\mathrm{d}}{\mathrm{d}x} (\bar{z}_{\mathrm{m}} F\Psi + \mu_m) \tag{3}$$

where partial densities have been replaced by concentrations. To reduce the amount of computation we deal with only one component. Then we can express the diffusion flow as:

$$J_{\pm} = -\frac{D_{\pm} c_{\pm}}{RT} \frac{\mathrm{d}}{\mathrm{d}x} (z_{\pm} F\Psi + \mu_{\pm}) = -\frac{D_{\pm} c_{\pm}}{RT} \frac{\mathrm{d}\mu_{\pm}}{\mathrm{d}x} \tag{4}$$

with $\mu_{\pm} = z_{\pm} F\Psi + \mu_{\pm}$.

The first term in the parentheses corresponds to the electrostatic and the second term to the chemical contributions. The symbol ± includes all positive and negative charge carrier effects.

Taking into account Einstein's law:

$$D_{\pm} = \bar{u}^{\pm}_{\text{abs}} kT$$

where $\bar{u}^{\pm}_{\text{abs}}$ is the absolute mobility and k the Boltzmann constant, and knowing that conventional mobility is defined by:

$$u_{\text{conv}} = \bar{u}^{\pm}_{\text{abs}} z_{\pm} e_0 \tag{5}$$

the diffusion flow can be written as:

$$J_{\pm} = \frac{\bar{u}^{\pm}_{\text{conv}} c_{\pm}}{z_{\pm} F} \frac{\mathrm{d}\mu_{\pm}}{\mathrm{d}x} \tag{6}$$

As can be seen from eqn. (6), diffusion flow depends not only on the chemical potential gradient and the concentration, but also on the ionic mobility. We can also see from eqn. (6) that a very low concentration would greatly reduce the diffusion flow and ionic transport will then become the reaction determining step. On the other hand, eqn. (6) represents the ionic flow due to "natural" diffusion in the absence of external forces. Assuming that the external electrical potential, load, forced flow, etc., are taking part in the general reaction, they increase ionic mobility and, in consequence, mass and charge transport between interphases are also increased.

Effect of circulation on charge transfer

(i) Influence on the structure of the double layer

We analysed the effect which electrolyte circulation from the bulk solution to the electrode through the interphase had on the charge transfer. Neglecting the transient state, in which flow depends on the initial concentration gradient, transport is determined by Fick's law. In the steady state $\vec{i}_{\text{CTR}} = \vec{i}_t$, where $\vec{i}_{\text{CTR}}$ and $\vec{i}_t$ are the inlet and outlet current to the interphase, respectively. As chemical processes are continuously removing ions from the bulk solution to the Outer Helmholtz Plate, however, the interphase structure does not remain in a steady state, its concentration varies as expressed by the following equation [5]:

$$C_{x,t} = C^0 - \frac{2J_D t^{1/2}}{D^{1/2}\pi^{1/2}} \exp(-x^2/4Dt) + J_D \frac{x}{D} \operatorname{cfer}(x/\sqrt{4Dt}) \tag{7}$$

where cfer is the error function given by

$$\operatorname{cfer}(u) = 2/\sqrt{\pi} \int \exp(-u^2)\, \mathrm{d}u \tag{8}$$

with x being the distance from the interphase plane in which we have

$$C_{0,t} = C^0 - \frac{2i_g}{nF} (t/\pi D)^{1/2} = C^0 - Pt^{1/2} \tag{9}$$

where $\vec{i}_g = nFJ_D$ is the total current, C^0 the initial concentration and

$$P = 2i_g/nF\sqrt{\pi D}. \tag{10}$$

From eqn. (9) (also called Sand's equation) we can see how the interphase concentration changes and the influence it has on the electrode covering and the reaction speed.

Nevertheless, as time passes and we move towards the steady state ($t \to \tau$), where τ is the transition time in which concentration becomes zero, $C^0 \to\!\!\to Pt^{1/2}$ and then $C_{0,t} \to\!\!\to 0$. In some cases (high concentration and low density current) τ takes high values and the electron acceptor becomes completely exhausted. Such a phenomenon will cause a gradient from the bulk solution to the near interphase, creating a natural convection flow tending to supply the removed charge from the Outer Helmholtz Plate.

The most important effect of convection–diffusion is to prevent the concentration near the interphase from being reduced to zero by the electron current. It also sets up a concentration gradient close to the interphase and acts as a variable thickness layer, depending on conditions. It can be written as follows:

$$\delta = 2(Dt/\pi)^{1/2} \tag{11}$$

and represents an important parameter because it has a great influence on both the overpotential and the current density. The diffusion layer thickness can be changed by forced convection.

(ii) Influence on the current density

The main influence the diffusion layer thickness has on the performance of an electrochemical device is that it determines the maximum current density ($\vec{i}_L$) which can be reached with fixed conditions. If we only consider natural diffusion and plate electrodes* we can express $\vec{i}_L$ as [5]

$$i_L = (DnF/\delta)C \tag{12}$$

where C is the charge carrier concentration.

We can see from eqn. (12) that $\vec{i}_L$ depends on δ. In general cases δ equals 5×10^{-2} cm; it gives, for D values of 10^{-5} cm^2 s^{-1}, an $\vec{i}_L$ value equal to 40 mA cm^{-2}, which is very low. If we try to increase the value of $\vec{i}_L$ we must reduce δ by at least one hundred fold; the easiest way is to reduce δ to one tenth, agitate the solution and consequently increase $\vec{i}_L$. Furthermore, as we are dealing with a number of different ions, and D depends on their respective mobilities, we can now define the transport coefficient either as a function of current density:

$$t_i = i_i/\Sigma i_i$$

or as a function of the mobilities

*We consider diffusion as a global reaction controller.

$t_i = u_i/\Sigma u_i$

In a pure diffusion process $t_i = 0$ and, taking into account other phenomena, eqn. (12) can be rewritten:

$$i_L = \frac{DnF}{1-t_i}\,\frac{C^0 - C_{0,t}}{\delta} = \frac{DnF}{\delta}\,C\,\frac{1}{1-t_i} \tag{12a}$$

where $C = C^0 - C_{0,t}$ and $0 < t < 1$.

As can be seen from eqn. (12a) $\vec{i}_L$ also increases with t_i.

Kappus and Bolhmann [6] have also demonstrated that current density depends proportionally on diffusive flow:

$$i_e = -2D_{ik}\{c(x_i) - [k_0(\eta)/k_1(\eta)]\}\mathrm{tgh}\{x_i[k_1(\eta)/D_{ik}]^{1/2}\} \tag{13}$$

for flat plates and

$$i_e = [k_1(\eta)D_{ik}]^{1/2}C(\eta)\{I_1[r_i(k_1(\eta)/D_{ik})^{1/2}]^- - \frac{I_1[r_j(k_1(\eta)/D_{ik})^{1/2}]}{k_1[r_j(k_1(\eta)/D_{ik})^{1/2}]}\,k_1[r_i(k_1(\eta)/D_{ik})^{1/2}]\} \tag{13a}$$

for tubular plates,

where

$k_0 = i_0 \exp(2F\eta\beta/RT)$

$k_1 = (i_0/C_0)\exp[-2F\eta(1-\beta)/RT]$

from the Butler–Volmer equation

and where

$\vec{i}_e$ represents the discharge current per plate of the limiting polarity
$c(x_i)$: acid concentration (in the boundary between active material zone and separator)
$\vec{i}_0$: specific exchange current
η : overvoltage
β : transfer coefficient
r_i : inner radius of the tubes
r_j : spine radius (tubular plates)
I_i : discharge current per cell
$K_1(z)$: modified Bessel function
$C(\eta)$: constant

and taking $D_{ik} = D_0\pi_{ij}^{\gamma}$ where D_0 is the pure diffusion coefficient, π_{ij} the porosity, and γ a variable parameter involving migration and electrolyte flow effects.

If we take into account the diffusion coefficient definition again, and we also consider migration and electrolyte flow effects, we can write, from eqn. (1):

$$D'_{ik} = \sum_{k=1}^{j-1} \Omega_{im} \frac{\partial \mu_m}{\partial \rho_k} + \sum_{k=1}^{j-1} \Omega_{im} \bar{F}_m$$

$$= \sum_{k=1}^{j-1} \Omega_{im} \left(\frac{\partial \mu_m}{\partial \rho_k} + \bar{F}_m \right) = D_{ik} + D^0_{ik} \tag{14}$$

The right hand side of the last expression supposes the new contribution and increases the D_{ik} value, increasing the output current according to eqns. (13) and (13a). We can also obtain the same result considering an effective increase in the porosity, making γ greater and increasing D_{ik}.

(iii) Influence on the reaction products

The electrolyte flow produces not only a "fictitious" growth in the porosity, but also a large reduction of the passivation layer on the electrode surface. As Winsel *et al.* [7] have demonstrated, a lead–acid cell can fail either by acid depletion in the pores or by $PbSO_4$ passivation layers on the electrode surface. Considering the latter problem, there are three different kinds of passivation: increased internal resistance (depending on the layer thickness only), limited diffusion flow to the electrode, and a $PbSO_4$ layer which prevents diffusion away from the electrode surface. The first two effects are insignificant but the last tends to passivate the electrode, preventing further reaction when the layer thickness equals $r/2$, where r is the pore radius. This layer also reduces the maximum current density which is given by:

$$i_L = \frac{F_{ik} D_{ik} c_i}{\lambda \delta_t} \tag{15}$$

where λ is the tortuosity.

As may be seen from eqn. (15) a large reduction in δ_t, removal of the passivation layer, increases $\vec{i}_L$ significantly.

Discharge processes

Figure 1 shows the experimental layout. Both cells start the discharge process from a state of maximum charge with the following initial conditions:

	Output voltage (V)	Density at upper zone (g cm^{-3})	Outer element discharge resistance (Ω)
Circulating system	2.126	1.260	0.262
Non-circulating system	2.128	1.256	0.265

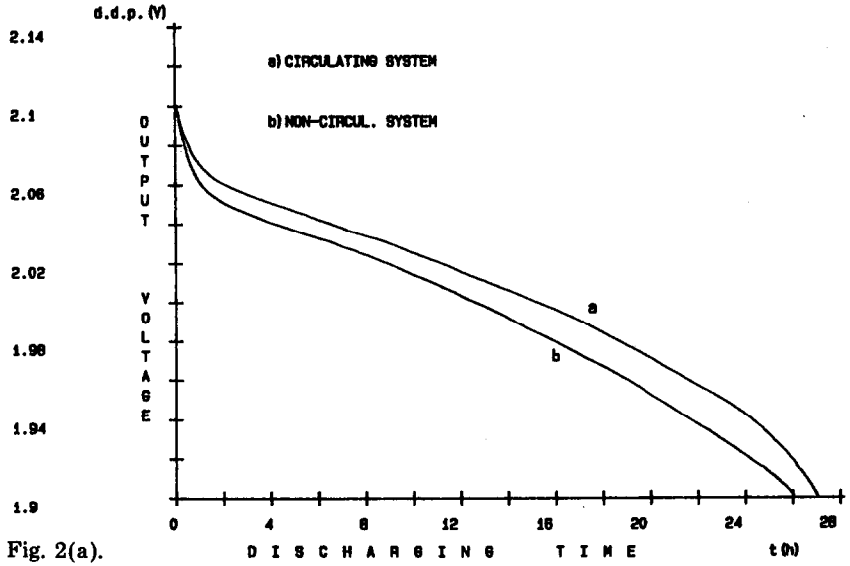

Fig. 2(a).

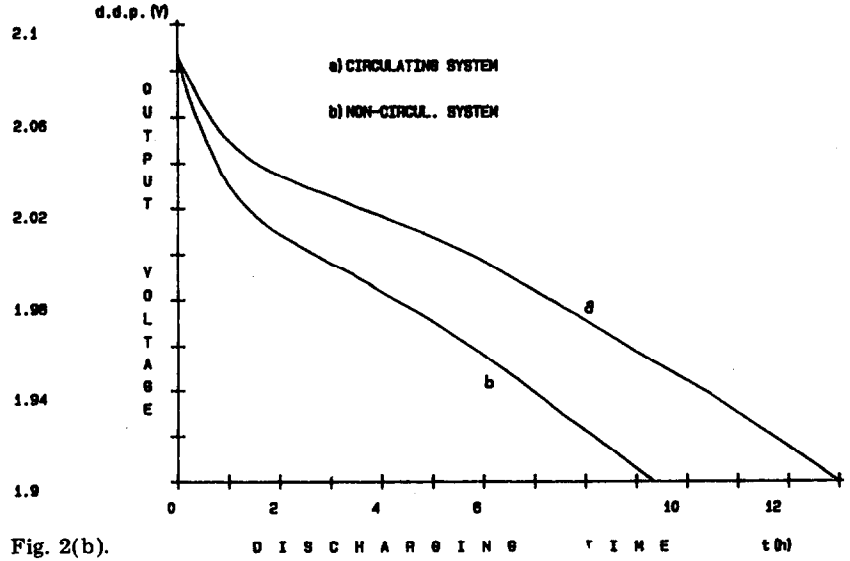

Fig. 2(b).

The circulating system density is homogeneous throughout the bulk solution and the resistance is constant over the discharge process. The discharge is ended when a previously determined voltage (1.9 V)* is reached.

Figure 2 shows discharge curves from both systems with the circulating electrolyte system giving a higher voltage over the whole range and taking

*FEMSA Mod. PTV 284/July 1984. Deutsche Normen DK 621.355.2-182.2 August, 1975.

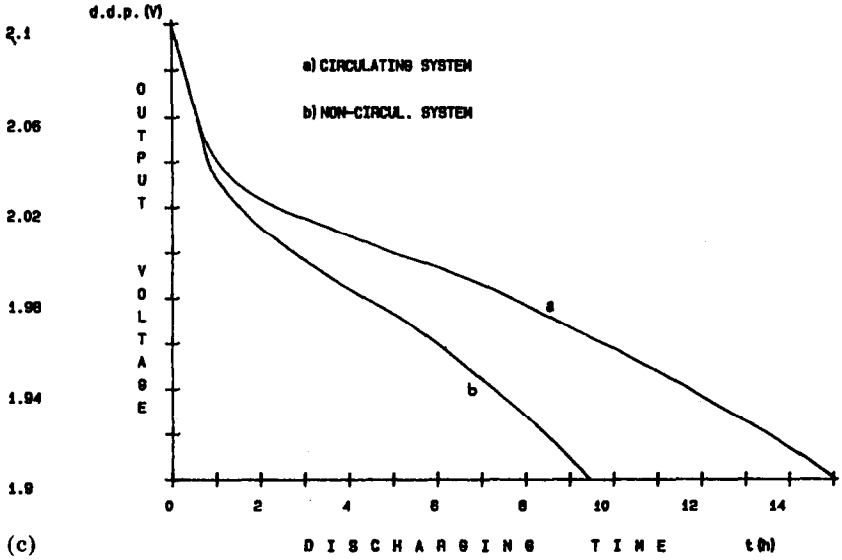

(c)

Fig. 2. Discharge voltage *vs.* time curves for two lead–acid cells. (a) Initial charge state 100%, right before gassing. (b) Initial charge state 80%. (c) Initial charge state 50%.

longer to fall to the cut-off voltage*. To calculate the total energy delivered from both "electrochemical sources" the voltage was integrated over time. The results were correlated to a straight line using regression analysis. The correlation with these results was good although for other curves the results were not so good. Voltage dependence on time from both devices gave the following expressions**:

$$V_1(t) = 2.076\,84 - 9.3 \times 10^{-5} t \tag{16}$$

$$V_2(t) = 2.067\,84 - 9.8 \times 10^{-5} t \tag{17}$$

with $r_1 = 0.972$ and $r_2 = 0.986$ being the respective regression coefficients.

We are able to calculate the total energy delivered given that:

$$E\,(\text{A h}) = \frac{1}{R} \int_{t_f}^{t_i} V(t)\,dt \tag{18}$$

and assuming R to be constant.

Using expressions (16) and (17) and integrating (18) we get:

$E_1 = 255$ A h; $E_2 = 230$ A h

*The cut-off time is given by the cut-off voltage depending on the total amount of energy delivered by a cell as a function of the discharging time according to specifications.

**From now on subscript 1 refers to the circulating cell and subscript 2 to the non-circulating cell.

As can be seen from these results the circulating electrolyte system supplies 11% more energy with the higher output voltage shown in Fig. 2.

Charge–discharge cycles

After confirming the viability of improving the lead–acid cell performance by means of electrolyte circulation we tested charge–discharge cycles to compare overall performance. The charging current was supplied from a continuous current source for some hours with both cells linked in series to ensure that both received the same energy. The charging half-cycle was ended at below maximum capacity because we wanted to compare charge–discharge cycles without the gas from the electrode reaction mixing up the layers in the unagitated cell. Thus, circulating and non-circulating systems show different initial conditions after charging. Stratification in the non-circulating system causes an inhomogeneous mass distribution, a voltage gradient, and capacity reduction. The discharge half-cycle was terminated at a fixed cut-off voltage (1.9 V).

In Table 1 we present a summary of the results from experiments using different initial conditions and different charging rates in circulating and non-circulating systems.

TABLE 1

Summary of results from charge–discharge tests of two lead–acid cells (with circulating and non-circulating electrolyte)

E (A h)	I_c (A)	t_c (h)	t_d (h)	η	$\Delta\eta$
23.0	2.0	11.5	2.8*	90.0*	18.7
			2.3	71.3	
29.1	5.4	5.4	4.25*	90.0*	18.2
			3.0	71.8	
78.0	3.0	26.0	7.0*	90.1*	17.1
			4.7	73.0	
91.6	5.6	10.5	13.0*	91.6*	16.2
	2.0	15.0	9.0	75.4	
110.2	5.8	19.0	15.0*	92.9*	15.8
			9.3	77.1	

E : Supplied charge during the charging half-cycle.
I_c : Charge current.
t_c : Charging time.
t_d : Discharging time.
η : Efficiency.
$\Delta\eta$: Efficiency improvement.
* : Circulating system.

Charging processes

The charging efficiency of both systems was measured to determine the improvement of performance due to electrolyte flow. The cells were first discharged to a known state given by voltage and density values (1.8 V and 1.150 g cm^{-3}). They were then both given the same charging current. Charging was maintained until the maximum charge states given by the greatest density and homogeneous solution for the unagitated battery, and up to that density value for the circulating system, were reached. To ensure that the circulating system had reached the final state, the maximum density value had to be kept constant for 3 h. Tests were carried out at different charge rates to establish the influence of the current on the cell performance.

We also measured the electromotive force of each cell by switching off the charge current and waiting for a few seconds to get a quasi-steady state.

Results

The results are plotted in Fig. 3(a), (b), and (c) and summarised in Table 2.

In Fig. 3(a) the cells were charged from the same initial conditions at a constant current of 2 A to the final state (homogeneous solution and maximum density). For Fig. 3(b) and (c) the charging rates were 4 A and 6 A, respectively. The density gradient between the top and the bottom in the unagitated battery after one or more charge–discharge cycles is due to

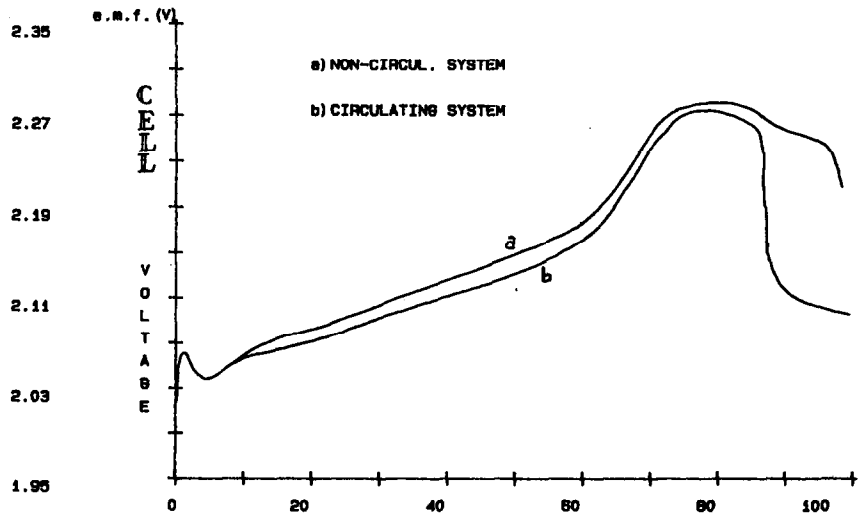

Fig. 3(a).

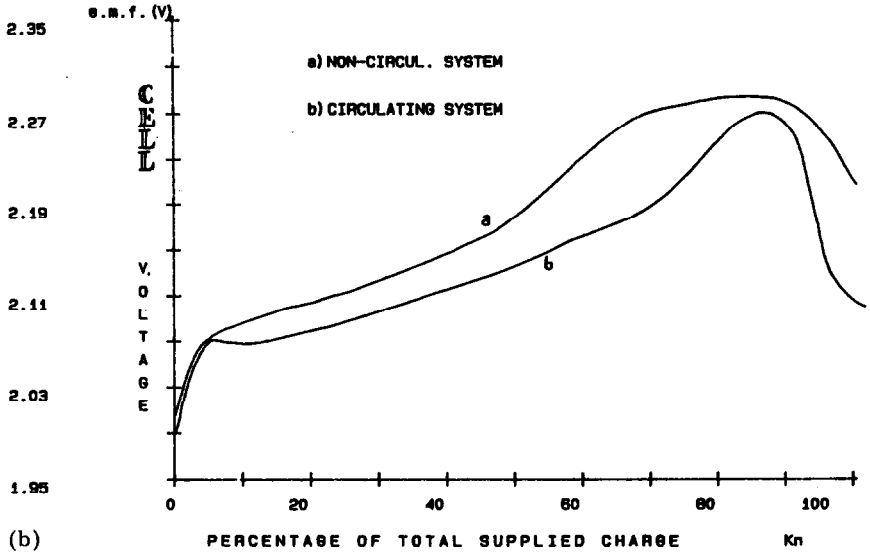

(b)

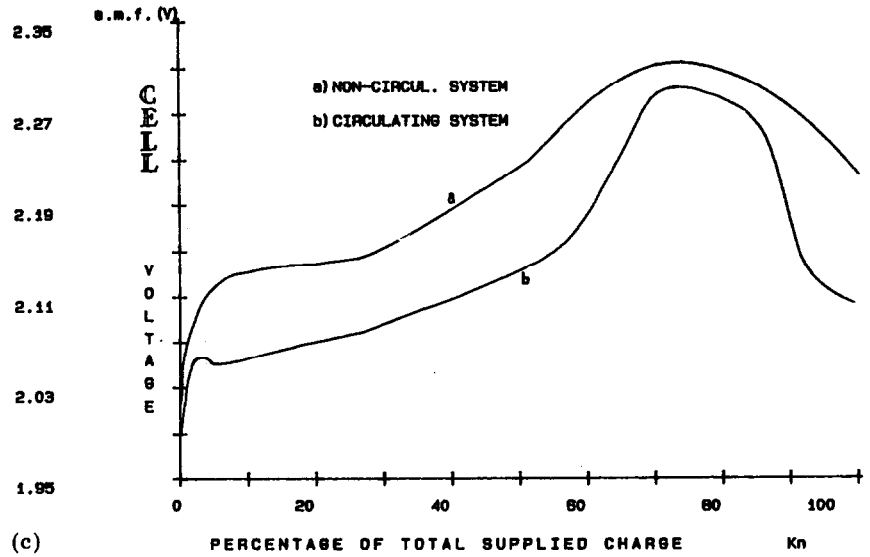

(c)

Fig. 3. Charging voltage *vs.* percentage of total charge in two lead–acid cells. (a) Charge rate at 2 A. (b) Charge rate at 4 A. (c) Charge rate at 6 A.

stratification created during the charge process, which remains during the discharge process. From the data we can obtain the total charge required to reach the final state by multiplying the current by the time.

If E_0 is the available energy from the maximum charge state and E_1, E_2 are the energies accepted by the circulating system and the unagitated

TABLE 2

Summary of results from charging processes in two lead–acid cells (circulating and non-circulating electrolyte)

E (A h)	I (A)	$\eta_{1,2}$ (%)	η'	$\Delta\eta$
149.0*	2.0	93.4*	76.0	22.4
195.5		71.0		
149.0*	4.0	93.1*	82.0	16.8
181.8		76.3		
149.0*	6.0	93.0*	85.5	13.5
174.0		79.5		

E : Charge supplied to the circulating system * and to the unagitated battery.
I : Charge current.
$\eta_{1,2}$: Efficiency.
η' : Efficiency ratio.
$\Delta\eta$: Efficiency improvement.

battery, respectively, during the charge process, the ratio of the efficiency of the systems is given by:

$$\eta' = \eta_2/\eta_1 = E_2/E_1 \tag{19}$$

where

$$\eta_1 = E_1/E_0 \text{ and } \eta_2 = E_2/E_0 \tag{20}$$

We can also define the charge saved by the circulating system as:

$$\Delta\eta = (\eta_1 - \eta_2) = (E_1/E_0 - E_2/E_0) = \eta_1(1 - E_2/E_1) = \eta_1(1 - \eta') \tag{21}$$

The graphs show the charging voltage as a function of the percentage of the total charge (K_n) in order that the results may be compared since different charges were supplied.

It can also be seen from Fig. 3 that the e.m.f. falls drastically at the end of the charging process. We believe that this effect is produced by transient phenomena due to secondary reactions, but further experiments are needed.

Test analysis

As can be seen from Table 1 the efficiency of the circulating system remains higher (between 16% and 19%) independently of both the charge state and the charge rate. Further efficiency values remain almost constant for all charge conditions.

The improvement in cell performance comes from a more homogeneous electrolyte mass distribution, enabling greater advantage to be taken of the

supplied energy, reducing energy losses and increasing capacity. It was shown, theoretically, in the first part of this paper, that passivation layers of $PbSO_4$ reduced the useful surface for electrode reaction by limiting the removal of the reaction products. General electrochemical processes suffer from this drawback with the penalty of reduced current and performance. On the other hand, inhomogeneous mass distribution in an unagitated cell causes current variations in the electrodes. Thus, the upper zones of plates in non-circulating systems suffer from high current densities, while the active material near the bottom suffers from being in concentrated acid. Furthermore, in non-circulating systems, the inhomogeneous current distribution creates higher voltages in the lower zones, increasing the c.e.m.f. and reducing the cell capacity.

From the data we can appreciate that the final voltage after charging is higher in a non-circulating cell with very low density and poorer performance. We can also see that the efficiency improvement is less as the state of charge increases, due to the gas which is generated stirring the electrolyte and tending to mix the layers, thus equalizing the performances.

We have also shown that the cell efficiency depends more on the state of the charge than on the charge rate, having obtained a 3 - 5% improvement in cell performance for the same charge rate. Further, Fig. 3(a), (b) and (c) shows that the circulating system homogenises more rapidly than does the unagitated battery. Moreover, the efficiencies of the charging processes are improved by reducing the charge rate, due to the creation of a chemical potential gradient as the current is increased and thereby limiting the capacity.

Conclusions

Electrolyte circulation improves the cycling performance and the efficiency of lead–acid batteries. The gain in efficiency is reduced, however, when the initial charge state is higher, becoming zero after "gassing" when the cell discharge performance does not depend on electrolyte circulation. The improvement obtained by using electrolyte flow is increased as the charge–discharge rate is reduced, due to the influence of diffusion phenomena. Most benefit can therefore be obtained from electrolyte circulation in batteries which are regularly cycled (daily) without being deeply discharged, thereby avoiding damage from a sustained low charge state and optimising the charge–discharge cycle efficiency. Circulation is more important during the charging half-cycle when stratification problems and density gradient become more evident.

List of symbols

C, c_k Concentration
$C(\eta)$ Constant

D_{ik} Relative diffusion coefficients
E Energy
F Faraday
F_m External forces
i Solute
i Current density
I Discharge current
J Diffusion flow
j Solvent
k Boltzmann constant
$K_1(z)$ Modified Bessel function
K_n Percentage of total supplied charge
n Number of charge carriers
r_i, r_j Radius
s_k Soret coefficient
T Absolute temperature
t Time
u Mobility
v_m Partial volumes
x Distance from the interphase plane
z_m Specific charge of ionic species, m
∇P Pressure gradient
∇T Temperature gradient
∇V Electrical potential gradient
β Transfer coefficient
λ Tortuosity
δ Diffusion layer thickness
η Efficiency
η' Overvoltage
$\Delta\eta$ Efficiency improvement
Ψ Electrostatic potential
π_{ik} Porosity
ρ Partial density
$\nabla\rho$ Partial density gradient
τ Transition time
μ Chemical potential
η' Relative efficiency
Ω_{im} Phenomenological coefficients

References

1 D. E. Bowman, Advanced lead–acid batteries, *Prog. Batteries Solar Cells, 5* (1984) 19 - 22.
2 K. Tomantschger, Effects of electrolyte agitation on the performance of lead–acid traction batteries at various temperatures, *J. Power Sources, 13* (1984) 137 - 149.
3 J. Fullea, A. Núñez and F. Graña, Nuevas perspectivas en acumuladores fotovoltaicos, *Mundo Electrónico, (Madrid), No. 163* (1986) pp. 101 - 108.

4 D. D. Fitts, *Nonequilibrium Thermodynamics*, McGraw-Hill, New York, 1962.
5 J. O'M. Bockris and A. K. N. Reddy, *Electroquímica Moderna*, Vols. I and II, Reverté, Barcelona, 1979.
6 W. Kappus and J. Bohmann, The influence of acid diffusion on the performance of lead–acid cells, *J. Power Sources, 10* (1983) 355 - 376.
7 A. Winsel, U. Hullmeine and E. Voss, Passivation reactions on the electrodes of a lead–acid cell, *J. Power Sources, 2* (1977/78) 369 - 385.

Suggested further reading

8 J. R. Pierson and C. E. Weinlein, Development of unique, lightweight, high-performance lead–acid batteries, *J. Power Sources, 9* (1982) 42 - 63.
9 P. Simons, *Storage Batteries*, Pitman, London, 1964.
10 H. J. S. Sand, *Philos. Mag., 1* (1900) 45.
11 W. Kappus and E. Voss, Recent lead–acid research at VARTA, *Prog. Batteries Solar Cells, 4* (1982) 187 - 191.
12 *Energía Solar Fotovoltàica*, Marcombo, Madrid, 1982.
13 D. Thuerk, Design of an efficient electrolyte circulation system for the lead–acid battery, *30th Power Sources Conf., Atlantic City, NJ, June, 1982.*
14 H. Bode, *Lead–Acid Batteries*, Wiley, New York, 1977.
15 K. J. Vetter, *Chem.-Ing.-Tech., 45* (1973) 213.
16 J. Bohmann, U. Hullmeine, E. Voss and A. Winsel, Active material structure related to cycle life and capacity, *Final Rep. ILZRO Project, LE-277*, VARTA Batterie AG.